ARCHIVES OF MECHANICS
Arch. Mech. **72** (2), 169–188, 2020, DOI: 10.24423/aom.3529

Static, free and forced vibration analysis of a delaminated microbeam-based MEMS subjected to the electrostatic force

A. RAZEGHI-HARIKANDEEI[1)], B. AZIZOLLAH GANJI[1)], R.-A. JAFARI-TALOOKOLAEI[2)], A. ABDIPOUR[3)]

[1)] *Department of Electrical and Computer Engineering, Babol Noshirvani University of Technology, 484 Babol, Iran, e-mails: razeghi.alieh@gmail.com, baganji@nit.ac.ir (corresponding author)*

[2)] *Department of Mechanical Engineering, Babol Noshirvani University of Technology, Babol, P.O. Box 47148-71167, Iran, e-mail: ra.jafari@nit.ac.ir*

[3)] *Microwave/mm-Wave and Wireless Communication Research Laboratory, Department of Electrical Engineering, Amirkabir University of Technology, 424 Hafez Ave, Tehran, Iran, e-mail: abdipour@aut.ac.ir*

In this paper, the delamination effect on the static and natural frequency response of a microbeam subjected to the nonlinear electrostatic force is studied using a semi-analytical approach for the first time. The Euler–Bernoulli beam assumption along with the non-classical modified couple stress theory is used to obtain the governing differential equation of motion and then a reduced-order model based on Galerkin's decomposition method is obtained. At first the microbeam with very small delamination like an intact microbeam is solved and then the solution is compared with those reported in the literature and the solution obtained using 3D-coupled electromechanical software. After validation, the effects of delamination length and its locations in thickness and length directions on the microbeam behavior are investigated in details. It is shown that the delamination has remarkable effects on the characteristics of the microbeam, especially near the pull-in voltage. Also, the delaminated microbeam with various thicknesses is studied using both the classical and the non-classical theories. It is found that the difference between the two models is significant for the thin microbeam with a thickness near of below than its material length scale parameter. This investigation is helpful for the nondestructive detection of the delamination in the beams.

Key words: microelectromechanical systems (MEMS), delaminated microbeam, static deflection, pull-in voltage, non-linear electrostatic force.

Copyright © 2020 by IPPT PAN, Warszawa

1. Introduction

The microelectromechanical system (MEMS) devices consist of microstructures such as beam and plate as the main part. This new technology is much desired in communication system applications due to their low loss devices such

as switches, phase shifters, antenna and resonators [1–3]. They are conventionally actuated using electrostatic force which is nonlinear along a beam or plate and causes the pull-in phenomenon. The sensitivity, frequency response, instability, distortion, and the dynamic range of these devices are related to the pull-in voltage and therefore their electromechanical analysis is very important.

The static deflection and the vibration of the intact microbeam around its statically deflected position under the electrostatic force due to a DC polarization voltage have been studied in many researches [4–9]. Abdel-Rahman *et al.* [4] have numerically studied the clamped-clamped microbeam under the action of an electrostatic force. The beam has been modeled as a distributed-mass structure and solved using a boundary-value problem. They have also presented a semi-analytical approach to investigate it in their next study and shown that their proposed reduced-order model can handle very stiff problems better than the previous method [5]. A reduced-order model based on the Differential Quadrature Method, Galerkin's decomposition method, and the finite-element model has been used by other researches for the pull-in voltage analysis [6–8]. In [9], the static behavior of electrostatically-actuated microbridges and microcantilevers has been investigated analytically using Galerkin's decomposition and the homotopy perturbation method.

In these studies, the well-known classical theories have been used to investigate the electrically actuated microbeams but the experimental observations have indicated that the deformation behavior in microscale structures is size-dependent in metals, polymers, and polysilicon [10]. Hence, several non-classical continuum theories such as strain gradient, modified couple stress, and Eringen's nonlocal elasticity theories, have been proposed for isotropic elastic materials in which the role(s) of material length-scale parameter(s) is (are) involved in the constitutive equations. Wang *et al.* [11] have used the strain gradient theory to model the electrostatically actuated microbeam-based MEMS for pull-in instability investigation. They also studied effects of surface energy on the pull-in instability of electrostatically actuated micro/nanoscale structures [12–14]. Miandoab *et al.* [15, 16] have used three non-classical continuum theories to estimate Young's modulus and non-classical parameters of polysilicon microbeam which leads to an appropriate agreement with experimental observation. Also, they have shown that the modified couple stress theory coincides experimental results better than Eringen's nonlocal elasticity and classical theories [16]. Moreover, the microbeam model based on the modified couple stress theory contains only an additional material constant, i.e., internal material length scale parameter l, unlike the strain gradient models and therefore, in the past decade, many researchers have studied the behavior of microbeams based on this novel and convenient theory [17–21].

All of the published researches have been dealt with the characterization of the intact electrostatically actuated structures using classical or non-classical

theory. On the other hand, the delamination (or through-the-width crack) can be created in the microbeam during their manufacturing process or service life and therefore studying the mechanical behavior of delaminated beams is new researches in literature. The behavior of delaminated beams can be studied based on the two well-known approaches, namely free and constrained models which have been presented by WANG *et al.* [22] and MUJUMDAR *et al.* [23], respectively. It is worth mentioning that the delaminated beam is divided into some intact beams i.e. sub-beams in which the delamination is their boundaries. In the constrained mode model, the sub-beams located in the delamination region are constrained to have the same transverse deflections, but in the free mode model, they are allowed to have different transverse deformations. Free vibrations of a delaminated beam have been studied in some references [24–26]. Likewise, there are studies on the transient response of the delaminated beams under the action of moving loads and oscillating masses [27–29]. All these publications studied macro delaminated beams. Recently, JAFARI-TALOOKOLAEI *et al.* [30] have presented the bending and vibration characteristics of a Bernoulli–Euler microbeam with single delamination using the non-classical modified couple stress theory.

To the best of authors' knowledge, there are no publications on the static and forced vibration analysis of the delaminated beam or microbeam under nonlinear electrostatic force using classical or non-classical theory. Hence, investigating the bending and vibration characteristics of a delaminated microbeam based on non-classical theory is the main contribution of the present work.

In this paper, the clamped-clamped microbeam is studied with single delamination subjected to a nonlinear electrostatic force distributed along its entire length. The delaminated microbeam is divided into four intact sub-beams. It is worth mentioning that two sub-beams located in the delamination region are assumed to move together (the constrained mode). We use a new non-classical model for Bernoulli–Euler beams which developed using the modified couple stress theory concept by PARK and GAO [31]. Then the static and vibration responses of the microbeam is studied for various parameters of the delamination. It is observed that the characteristics of the delaminated microbeam are very sensitive to that length and location. Also, the delaminated microbeam with various geometrical parameters is studied based on classical and non-classical Euler–Bernoulli models. It is shown that the difference between the two models is significant for microbeams with small thickness.

2. Problem definition and formulation

The considered microbeam with a rectangular cross-section of $b \times h$ and length of L under the electrostatic force is shown in Fig. 1. Referring to Fig. 2, the delaminated microbeam is divided into four intact sub-beams. The microbeam

has single delamination with length of L_d located at a distance of L_1 from the microbeam's left end and height of h_2 from the top surface (see Fig. 2). The electrostatic force creates a distributed force per unit length of the microbeam as below [32]:

$$F(V,W) = \frac{1}{2}\varepsilon b \frac{V^2}{(d - W(x,t))^2} \tag{2.1}$$

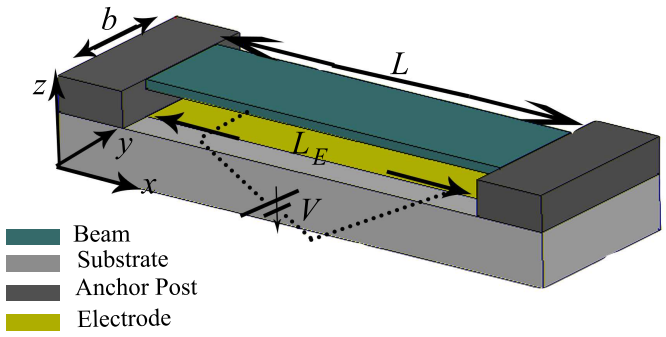

FIG. 1. The schematic view of the delaminated microbean.

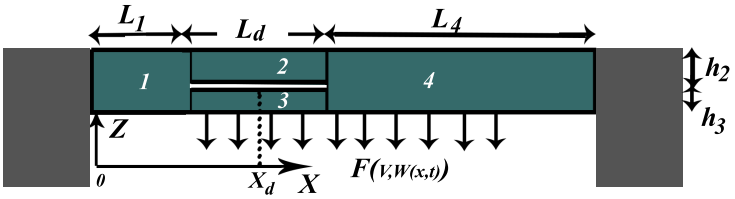

FIG. 2. Representation of a delaminated microbeam.

where ε is the dielectric constant of the gap between two electrodes and d is the distance between the fixed and the movable electrodes. Likewise, V is an applied voltage which is constant and independent of the time (DC). The symbol of $W(x,t)$ is the microbeam's deflection. We assume that the delaminated microbeam consisted of four intact sub-beams and two sub-beams located in the delamination region move together (the constrained mode proposed in [23] i.e. $W_2 = W_3$). Afterwards, we use the new model for the bending of a Bernoulli–Euler beam developed using a non-classical modified couple stress theory by PARK and GAO [31] for the first time. They showed that the bending deformation of the beam has two contributions: one associated with the normal stress component (the conventional term); and the other associated with the couple

stress component (the additional term). They indicated that the bending rigidity of the beam is equal to $D = EI + \mu Al^2$ which explicitly depends on internal material length scale parameter of l. This beam model based on the modified couple stress theory contains only one additional material constant (l), unlike the other non-local beam models. Nevertheless, the presence of l enables the incorporation of the material microstructural features in the new model and renders it possible to explain the size effect, unlike the classical Bernoulli–Euler beam model. Based on this non-classical model and according to the constrained mode model, the equation of motion of i^{th} sub-beams can be written as below (the readers are referred to [30] for more in-depth discussion of this equation):

$$D_i W_i''''(x,t) + m_i \ddot{W}_i(x,t) = F(V, W(x,t)) \quad (i = 1 \text{ and } 4), \tag{2.2a}$$

$$(D_2 + D_3) W_2''''(x,t) + (m_2 + m_3) \ddot{W}_2(x,t) = F(V, W(x,t)), \tag{2.2b}$$

where:

$$D_i = EI_i + \mu A_i l^2 \tag{2.3}$$

in which prime ($'$) and dot ($\dot{}$) denote the derivative of W with respect to the spatial coordinate (x) and time (t), respectively. Besides, E is Young's modulus, μ is the shear modulus, and l is the length scale parameter of the microbeam. Likewise, I_i and m_i are the moment of inertia and mass per unit length of the i^{th} sub-beam, respectively. I_i and m_i can be written as:

$$I_i = bh_i^3/12, \quad m_i = \rho A_i, \tag{2.4}$$

where ρ is the density of the microbeam and A_i is the i^{th} sub-beam cross section area.

A close inspection of Eq. (2.2b) reveals that the constrained mode model has been considered for sub-beams 2 and 3. In the constrained mode model, the sub-beams located in the delamination region are constrained to have the same transverse deflections. The clamped-clamped boundary conditions are assumed for the delaminated microbeam. These conditions can be written as:

$$W_1(0,t) = 0, W_1'(0,t) = 0, \quad W_4(L,t) = 0, \quad W_4'(L,t) = 0. \tag{2.5}$$

The following continuity conditions of the transverse deflection have to be considered for the sub-beam 2 (see Fig. 2):

$$W_1(L_1,t) = W_2(L_1,t), W_2(L_1 + L_d, t) = W_4(L_1 + L_d, t). \tag{2.6}$$

The continuity conditions of the slope are as:

$$W_1'(L_1,t) = W_2'(L_1,t), \quad W_2'(L_1 + L_d, t) = W_4'(L_1 + L_d, t), \tag{2.7}$$

the compatibility conditions of the shear forces are:

$$\begin{aligned} D_1 W_1'''(L_1,t) &= (D_2+D_3)W_2'''(L_1,t), \\ D_4 W_4'''(L_1+L_d,t) &= (D_2+D_3)W_2'''(L_1+L_d,t), \end{aligned} \tag{2.8}$$

the equilibrium conditions for the bending moments by considering the axial force are obtained as [28]:

$$\begin{aligned} D_1 W_1'' L_1,t) &= (D_2+D_3)W_2''(L_1,t) \\ &\quad - \frac{h_1^2}{4L_d}\left[\frac{W_1'(L_1,t)-W_4'(L_1+L_d,t)}{\frac{1}{E_2A_2}+\frac{1}{E_3A_3}}\right], \end{aligned} \tag{2.9}$$

$$\begin{aligned} D_4 W_4''(L_1+L_d,t) &= (D_2+D_3)W_2''(L_1+L_d,t) \\ &\quad - \frac{h_1^2}{4L_d}\left[\frac{W_1'(L_1,t)-W_4'(L_1+L_d,t)}{\frac{1}{E_2A_2}+\frac{1}{E_3A_3}}\right]. \end{aligned} \tag{2.10}$$

For convenience, we introduce the non-dimensional variables (denoted by hat) as:

$$\hat{x} = \frac{x}{L}, \quad \hat{t} = \frac{t}{T}, \quad \hat{W}(\hat{x},\hat{t}) = \frac{W(x,t)}{d}, \tag{2.11}$$

where $T = (\rho b h_1 L^4/D_1)^{1/2}$. By substituting Eq. (2.11) into Eq. (2.2), the normalized governing equations of the motion of four sub-beams are obtained:

$$\hat{W}_i''''(\hat{x},\hat{t}) + B_i \ddot{\hat{W}}_i(\hat{x},\hat{t}) = R_i \frac{V^2}{(1-\hat{W}_i(\hat{x},\hat{t}))^2}, \tag{2.12}$$

$$B_i = \begin{cases} \dfrac{m_i}{D_i}\dfrac{L^4}{T^2} & (i=1 \text{ and } 4), \\ \dfrac{m_2+m_3}{D_2+D_3}\dfrac{L^4}{T^2} & (i=2 \text{ and } 3), \end{cases}$$

$$R_i = \begin{cases} \dfrac{1}{D_i}\dfrac{b\varepsilon L^4}{2d^3} & (i=1 \text{ and } 4), \\ \dfrac{1}{D_2+D_3}\dfrac{b\varepsilon L^4}{2d^3} & (i=2 \text{ and } 3). \end{cases} \tag{2.13}$$

3. Free vibration

The microbeam is assumed as a system with finite degrees of freedom using the Galerkin decomposition method. Based on this method, the deflection of the microbeam can be written as the multiplication of the spatial and time parts:

$$\hat{W}_i(\hat{x},\hat{t}) = \sum_{k=1}^{n} \Phi_{ik}(\hat{x}) q_k(\hat{t}) \tag{3.1}$$

where Φ_{ik}(x) is the basis function of the i^{th} sub-beam for the k^{th} mode and q_k(t) is its time-dependent part. The $q_k(t)$ is not defined with index i because it is the same for all sub-beams. The four sub-beams are assumed to move harmonically in the initial situation without applied force as:

$$\hat{W}_i(\hat{x},\hat{t}) = \Phi_{ik}(\hat{x})\sin(\omega_k \hat{t}), \tag{3.2}$$

where ω_k is the natural frequency of the delaminated microbeam proportional to the k^{th} mode of free vibration. The above assumption is substituted in Eq. (2.12) and then is solved for the zero applied voltage. The basis function is calculated as:

$$\begin{aligned}\Phi_{ik}(\hat{x}) = {} & s_i \sin(B_i\sqrt{\omega_k}\hat{x}) + c_i \cos(B_i\sqrt{\omega_k}\hat{x}) \\ & + sh_i \sinh(B_i\sqrt{\omega_k}\hat{x}) + ch_i \cosh(B_i\sqrt{\omega_k}\hat{x}).\end{aligned} \tag{3.3}$$

The four unknown constant parameters of the s_i, c_i, sh_i, and ch_i of the i^{th} sub-beam and the natural frequency of the k^{th} mode of the microbeam is obtained by substituting Eq. (3.2), using Eq. (3.3), into twelve boundary conditions described in Eqs. of (2.5)–(2.10).

4. Static behavior

When a DC voltage, V_s, is applied, the microbeam deflects in a static position and therefore the movement for the static response is independent of the time and it can be assumed as follows:

$$\hat{W}_{is}(\hat{x}) = \sum_{k=1}^{n} \Phi_{ik}(\hat{x}) q_{sk} \tag{4.1}$$

in which the linear-undamped mode shape, Φ_{ik}, obtained in last section is used. The index of s shows the static state. Thus, the microbeam is described in the static state using (2.12) without time part dependency as:

$$(1-\hat{W}_{is}(\hat{x}))^2 \hat{W}''''_{is}(\hat{x}) = R_i V_s^2. \tag{4.2}$$

Equation (4.1) is substituted in the above equation, using (3.3),and then it is multiplied with Φ_{ik}. Next, we integrate the outcome equation from $\hat{x} = 0$ to 1 ($0 < x < L$) (through the normalized length of the microbeam). It is noticed that overall integral consisted of three section of $0 < x < L_1$, $L_1 < x < L_{1+}L_d$ and $L_{1+}L_d < x < L$ proportional to each sub-beams. The k non-linear algebraic

equations are obtained as:

$$
\begin{aligned}
(4.3)\qquad & \int_{0}^{L1/L} \Phi_{1k}(\hat{x})\Big[1-2\sum_{k=1}^{n}\Phi_{1k}(\hat{x})q_{sk}+\Big(\sum_{k=1}^{n}\Phi_{1k}(\hat{x})q_{sk}\Big)^2\Big]\sum_{k=1}^{n}\Phi''''_{1k}(\hat{x})q_{sk}d\hat{x}\\
&+\int_{L1/L}^{(L1+Ld)/L} \Phi_{2k}(\hat{x})\Big[1-2\sum_{k=1}^{n}\Phi_{2k}(\hat{x})q_{sk}+\Big(\sum_{k=1}^{n}\Phi_{2k}(\hat{x})q_{sk}\Big)^2\Big]\sum_{k=1}^{n}\Phi''''_{2k}(\hat{x})q_{sk}d\hat{x}\\
&+\int_{(L1+Ld)/L}^{1} \Phi_{4k}(\hat{x})\Big[1-2\sum_{k=1}^{n}\Phi_{4k}(\hat{x})q_{sk}+\Big(\sum_{k=1}^{n}\Phi_{4k}(\hat{x})q_{sk}\Big)^2\Big]\sum_{k=1}^{n}\Phi''''_{4k}(\hat{x})q_{sk}d\hat{x}\\
&=V_s^2\Big[\int_{0}^{L1/L} R_1\Phi_{1k}(\hat{x})+\int_{L1/L}^{(L1+Ld)/L} R_2\Phi_{2k}(\hat{x})+\int_{(L1+Ld)/L}^{1} R_4\Phi_{4k}(\hat{x})\Big]d\hat{x}.
\end{aligned}
$$

The above equation is numerically solved to obtain q_{sk} and then the static response of the microbeam is determined using (4.1).

5. Forced vibration

It is interesting to study the natural frequency variation of the delaminated microbeam versus the different applied DC voltages. Hence, we assume that the microbeam has static deflection with a very small variation around it as:

$$
(5.1)\qquad \hat{W}_i(\hat{x},\hat{t})=\sum_{k=1}^{n}\Phi_{ik}(\hat{x})q_k(\hat{t})=\sum_{k=1}^{n}\Phi_{ik}(\hat{x})(q_{sk}+q_{dk}(\hat{t})).
$$

In which the linear-undamped mode shape, Φ_{ik}, and q_{sk} obtained in the last section is used. The q_{dk} is the dynamic component with a very small magnitude around static equilibrium. Equation (2.12) is rearranged and the normalized governing equation of the motion in the dynamic behavior is obtained as below:

$$
(5.2)\qquad (1-\hat{W}_i(\hat{x},\hat{t}))^2\hat{W}_i''''(\hat{x},\hat{t})+B_i(1-\hat{W}_i(\hat{x},\hat{t}))^2\ddot{\hat{W}}_i(\hat{x},\hat{t})=R_iV_s^2.
$$

Equation (5.1) along with Eq. (3.3) is substituted in the above equation and then it is multiplied with $\Phi_{ik}(x)$. Next, we integrate the outcome equation from $\hat{x}=0$ to 1 ($0<x<L$) (through the normalized length of the microbeam). It is noticed that overall integral consisted of three section of $0<x<L_1$, $L_1<x<L_{1+}L_d$ and $L_{1+}L_d<x<L$ proportional to each sub-beams. The k non-linear algebraic equations are obtained as below:

$$
\begin{aligned}
(5.3)\qquad &+B_1\int_0^{L1/L}\Phi_{1k}(\hat{x})\Big[1-2\sum_{k=1}^{n}\Phi_{1k}(\hat{x})q_k(\hat{t})+\Big(\sum_{k=1}^{n}\Phi_{1k}(\hat{x})q_k(\hat{t})\Big)^2\Big]\sum_{k=1}^{n}\Phi_{1k}(\hat{x})\ddot{q}_k(\hat{t})d\hat{x}\\
&+B_2\int_{L1/L}^{(L1+Ld)/L}\Phi_{2k}(\hat{x})\Big[1-2\sum_{k=1}^{n}\Phi_{2k}(\hat{x})q_k(\hat{t})+\Big(\sum_{k=1}^{n}\Phi_{2k}(\hat{x})q_k(\hat{t})\Big)^2\Big]\sum_{k=1}^{n}\Phi_{2k}(\hat{x})\ddot{q}_k(\hat{t})d\hat{x}\\
&+B_4\int_{(L1+Ld)/L}^{1}\Phi_{4k}(\hat{x})\Big[1-2\sum_{k=1}^{n}\Phi_{4k}(\hat{x})q_k(\hat{t})+\Big(\sum_{k=1}^{n}\Phi_{4k}(\hat{x})q_k(\hat{t})\Big)^2\Big]\sum_{k=1}^{n}\Phi_{4k}(\hat{x})\ddot{q}_k(\hat{t})\\
&+\int_0^{L1/L}\Phi_{1k}(\hat{x})\Big[1-2\sum_{k=1}^{n}\Phi_{1k}(\hat{x})q_k(\hat{t})+\Big(\sum_{k=1}^{n}\Phi_{1k}(\hat{x})q_k(\hat{t})\Big)^2\Big]\sum_{k=1}^{n}\Phi''''_{1k}(\hat{x})q_k(\hat{t})d\hat{x}\\
&+\int_{L1/L}^{(L1+Ld)/L}\Phi_{2k}(\hat{x})\Big[1-2\sum_{k=1}^{n}\Phi_{2k}(\hat{x})q_k(\hat{t})+\Big(\sum_{k=1}^{n}\Phi_{2k}(\hat{x})q_k(\hat{t})\Big)^2\Big]\sum_{k=1}^{n}\Phi''''_{2k}(\hat{x})q_k(\hat{t})d\hat{x}\\
&+\int_{(L1+Ld)/L}^{1}\Phi_{4k}(\hat{x})\Big[1-2\sum_{k=1}^{n}\Phi_{4k}(\hat{x})q_k(\hat{t})+\Big(\sum_{k=1}^{n}\Phi_{4k}(\hat{x})q_k(\hat{t})\Big)^2\Big]\sum_{k=1}^{n}\Phi''''_{4k}(\hat{x})q_k(\hat{t})d\hat{x}\\
&\qquad=V_s^2\Big[\int_0^{L1/L}R_1\Phi_{1k}(\hat{x})+\int_{L1/L}^{(L1+Ld)/L}R_2\Phi_{2k}(\hat{x})+\int_{(L1+Ld)/L}^{1}R_4\Phi_{4k}(\hat{x})\Big]d\hat{x}.
\end{aligned}
$$

The above k algebraic equations are rearranged as below [33]:

$$\ddot{q}=F(q), \tag{5.4}$$

where F is vector-valued function of $q=[q_1,q_2,\ldots,q_k]$. Then the linearized equation is obtained after expressing the function $F(q)$ in Taylor series, and neglecting the higher order terms as $\ddot{q}_d=J(q_s)q_d$; J is also the Jacobian matrix of function F. Afterwards, the natural frequency related to the applied DC voltage, V_s, is calculated using square root of the eigenvalues of the matrix at the related static position of q_s.

6. Numerical results

6.1. Verification

In order to verify our model, the static response of the microbeam with small delamination of $L_d=0.001L$ like an intact microbeam is calculated for different static forces (or different Vs) and compared with the result reported by CHOI and LOVELL [34] and the three dimensional coupled electro-mechanical solution achieved using a commercially available software IntelliSuite$^{\mathrm{TM}}$ in Fig. 3. The

considered intact microbeam made of polysilicon ($E = 165$ GPa) has geometrical properties of $L = 400\,\mu$m, $b = 45\,\mu$m, $h = 2\,\mu$m, and $d = 1\,\mu$m such as studied in [34]. Also, the length scale parameter of the polysilicon is not considered and it is set to zero to use classical theory for the sake of comparison. The numerical result is obtained for maximum deflection of the microbeam for one, two, three, four, and five terms of the series solution and shown in Fig. 3. The results demonstrate that they are converged with increasing the number of truncated terms in the series. As shown in Fig. 3, the five terms discretization result approximately coincides with the three terms discretization solution and they are in excellent agreement with the solutions presented by [34] and the 3D electromechanical software. It can be concluded that the five-term discretization is sufficient to investigate the microbeam under electrostatic force using the proposed approach. Also, it is observed, in Fig. 3, that two and four-mode discretization results are similar to one and three-mode solutions respectively. It is concluded that the mode discretization solution with the odd number is better to model the fixed-fixed symmetrical beam problems. In other words, the even-mode basis functions are unsymmetric and does not affect the response because the microbeam maintains a symmetric shape during motion. In the following, we investigate the delamination effect on the static deflection, the free and forced vibration behavior of the microbeam based on the non-classical theory along with three-mode Galerkin's decomposition method. The length scale parameter of polysilicon is set to $l = 0.17\,\mu$m [16].

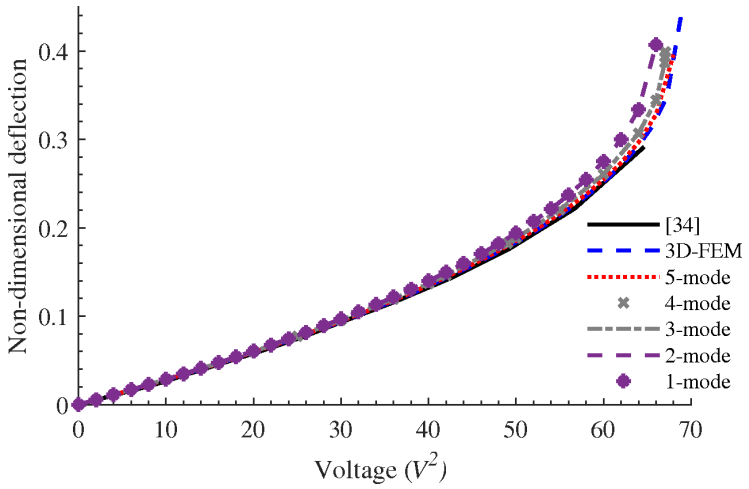

Fig. 3. Comparison of the maximum non-dimensional deflection of the intact microbeam which has been solved using the proposed approach (one, two, three, four, and five-mode) with the numerical result reported by Choi and Lovell [34] and the 3D coupled electro-mechanical solution obtained using IntelliSuite^{TM}.

6.2. Static deflection

First the central delamination is considered i.e. $h_2 = 0.5h$, $x_d = 0.5L$. In Fig. 4, the static response is displayed for different delamination lengths. The results show that the delamination leads to an increase in the maximum deflection of the microbeam in comparison to intact microbeam. The delamination has an insignificant effect on the response of the microbeam at low electrostatic force (applied voltage), but by increasing the voltage, its significant influence is observed. It is important to note that from the mathematical point of view, where the derivative of the maximum deflection is infinite, the pull-in phenomena will happen [9]. In this voltage, the microbeam is not stable and the microbeam is forced to be in contact with the substrate. The results show that the pull-in voltage decreases when delamination length increases. It is indicated that the delamination effect in the capacitive microbeam sensors which should be work below the pull-in voltage such as microphone is impressively high [35].

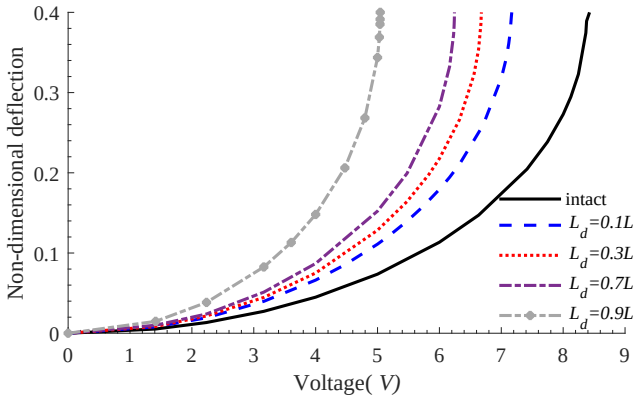

FIG. 4. The static response of the maximum non-dimensional deflection of the microbeam with central delamination ($h_2 = 0.5h$ and $x_d = 0.5L$) with different lengths.

In the next study, the delamination with lengthwise location $x_d = 0.5L$, $L_d = 0.1L$, and different vertical locations $h_2 = 0.1h$, $0.3h$, $0.4h$, and $0.5h$ is considered and the maximum non-dimensional deflection of the microbeam versus different DC voltage is solved and shown in Fig. 5. The deflection decreases when the delamination occurs far away from the microbeam's mid-plane related to the thickness and therefore the pull-in phenomenon occurs in higher voltage. Also, it is important to note that owning to vertical symmetry, the movement behavior of the microbeam for the vertical locations of $h_2 = 0.9h$, $0.7h$, and $0.6h$ are equal to the $h_2 = 0.1h$, $0.3h$, and $0.4h$, respectively.

Next, the lengthwise location of the delamination on the static response of the delaminated microbeam is investigated in Fig. 6. The microbeam with the

delamination length $L_d = 0.1L$, vertical location $h_2 = 0.5h$ and different lengthwise location $x_d = 0.1L$, $0.3L$, and $0.5L$ is considered. The results show that the microbeam with the delamination with the central lengthwise location has more deflection than the other with delamination near to the end of the microbeam. Also, it is observed that the response related to different lengthwise location is not regular due to the variation of overall stiffness that is also observed in other researches like [36, 37].

Finally, it is interesting to study the classical theory limitation to be responsible for microbeam behavior. Thus the maximum static deflection of four

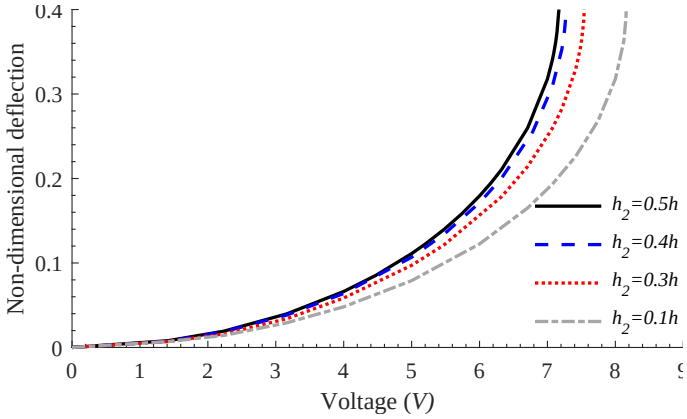

FIG. 5. The static response of the maximum non-dimensional deflection of the microbeam with delamination with lengthwise location $x_d = 0.5L$, $L_d = 0.1L$, and different vertical location of $h_2 = 0.1h$, $0.3h$, $0.4h$, and $0.5h$.

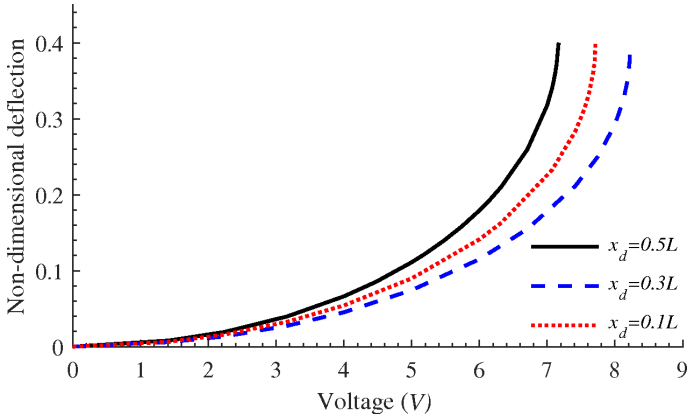

FIG. 6. The maximum non-dimensional deflection of the microbeam with delamination with length of $0.1L$ located in the center of the microbeam in vertical location ($h_2 = 0.5h$) with different lengthwise location ($x_d = 0.1L$, $0.3L$, and $0.5L$).

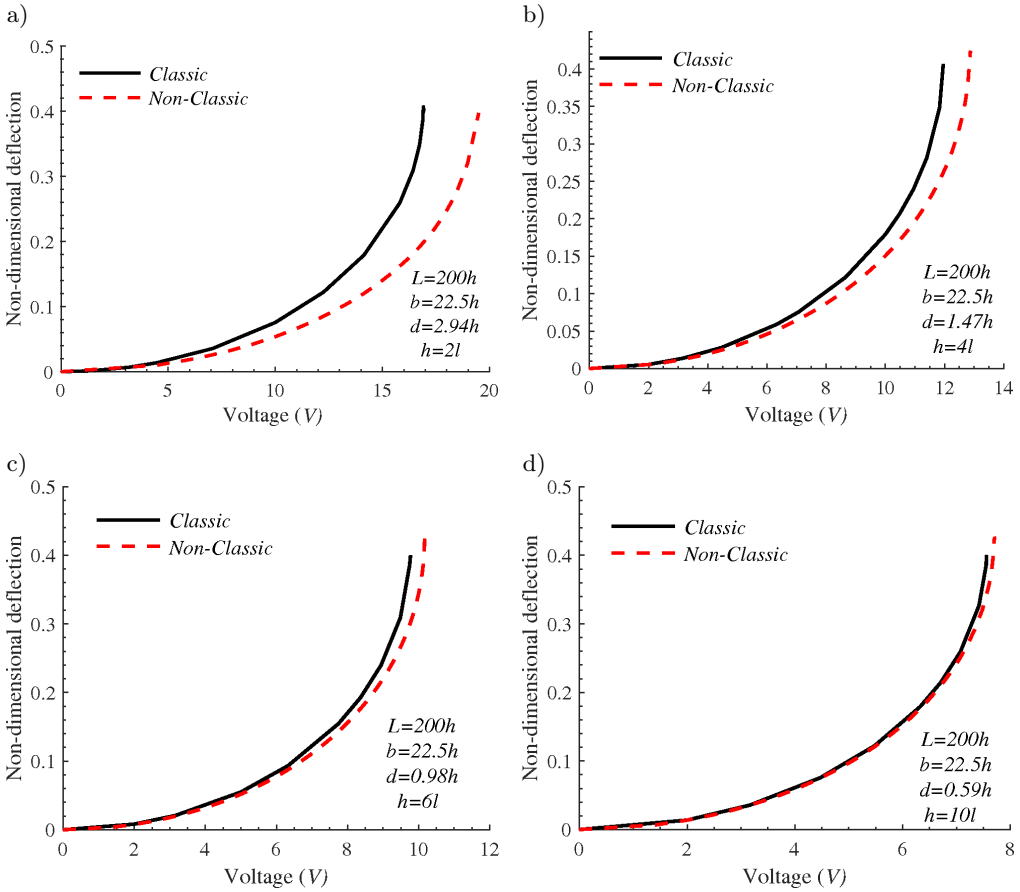

FIG. 7. The maximum non-dimensional deflection of the delaminated microbeam ($x_d = 0.5L$, $h_2 = 0.5h$, and $L_d = 0.1L$) based on the classic and the non-classic theory with various thickness; a) $h = 2l$, b) $h = 4l$, c) $h = 6l$ and d) $h = 10l$.

different microbeams with the various thicknesses ($h = 2l$, $4l$, $6l$, and $10l$) with the constant ratio of the length and the width to the thickness are studied and the solution results have been shown in Fig. 7. The results show that only the non-classical theory should be used to study the very thin microbeams with $h/l < 10$. The classical theory is approximately responsible for the behavior of the microbeam below the pull-in instability operation for the h/l ratio lower than 10 and near to 6 (Fig. 7c). But the exact estimation of the classical theory only occurs in the thick microbeams with $h/l > 10$.

6.3. Free and forced vibration

The fundamental frequency variation of the delaminated microbeam versus different applied DC voltage is studied here. First, the microbeam with central

Table 1. The fundamental frequency of the delaminated microbeam with various length ($h_2 = 0.5h$ and $x_d = 0.5L$) at rest ($V_s = 0$).

Delamination length, L_d	intact	$0.1L$	$0.3L$	$0.7L$	$0.9L$
Fundamental frequency [KHz]	109.562	95.980	88.463	81.599	65.876

delamination i.e. $h_2 = 0.5h$, $x_d = 0.5L$ with different length is studied. The variation of the fundamental frequency for the non-actuated microbeam ($V_s = 0$) is shown in Table 1. It is observed that the delamination has a high effect on the natural frequency value of the intact microbeam. When the delamination length increases, the natural frequency decreases. The fundamental frequency variation with different applied voltage is illustrated in Fig. 8 in which the pull-in phenomenon is demonstrable in the natural frequency behavior. Mathematically for the pull-in instability, the natural frequency will be zero that is reasonable because the microbeam reaches to substrate with no motion. It is shown when the applied voltage increases, the delamination effect on the fundamental frequency reduction increases that cause the pull-in phenomenon occurs in lower voltage for the microbeam with longer delamination.

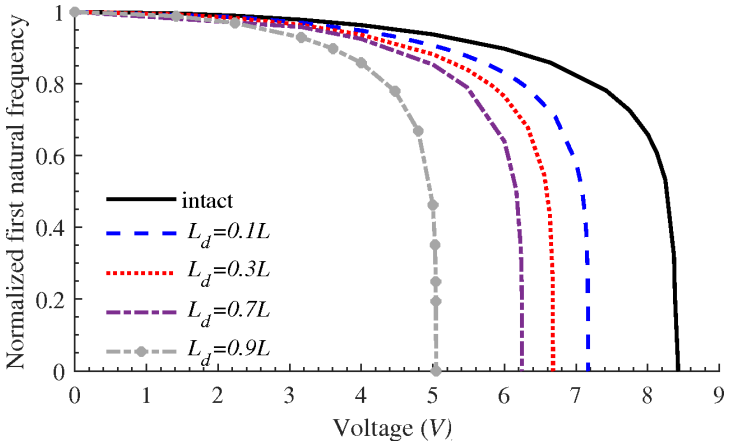

FIG. 8. The influence of delamination length on the fundamental frequency of the delaminated microbeam ($h_2 = 0.5h$ and $x_d = 0.5L$).

The effect of vertical location of the delamination on the fundamental frequency for the microbeam at rest ($V_s = 0$) is shown in Table 2. Delamination's

Table 2. The fundamental frequency of the delaminated microbeam with various vertical location ($L_d = 0.1L$ and $x_d = 0.5L$) at rest ($V_s = 0$).

Thicknesswise location, h_2	0.5h	0.4	0.3h	0.1h
Fundamental frequency [KHz]	95.980	98.239	100.305	107.154

length is set to $0.1L$ and located at the microbeam center ($x_d = 0.5L$). Besides, four vertical locations of $h_2 = 0.1h, 0.3h, 0.4h$, and $0.5h$ are considered. It is observed that when the delamination occurs near to the surface of the microbeam the fundamental frequency increases. Figure 9 shows the effect of vertical location of the delamination on the fundamental frequency variation versus different applied voltage. It can be seen from Fig. 9, when the delamination comes near to the surface of the microbeam, the natural frequency increases and therefore the pull-in voltage occurs in a higher value.

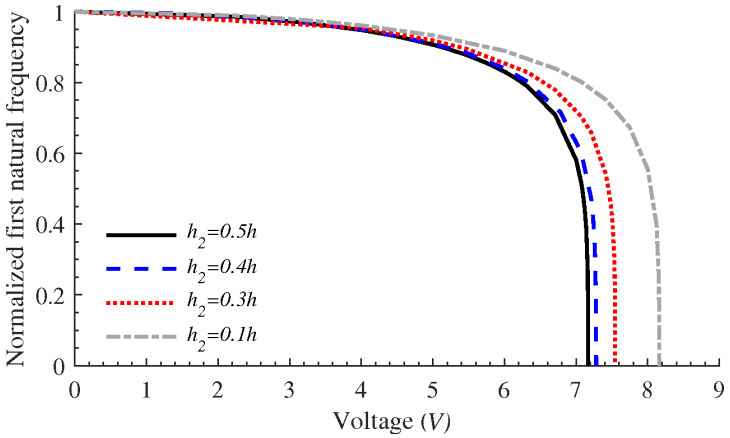

FIG. 9. The effect of vertical location of the delamination on the fundamental frequency of a delaminated microbeam ($L_d = 0.1L$ and $x_d = 0.5L$).

Additionally, the lengthwise location effect of the delamination on the fundamental frequency of the delaminated microbeam is investigated in Table 3 and Fig. 10. It is assumed that delamination has a length of $0.1L$ and is vertically located at $h_2 = 0.5h$. Three lengthwise locations of $x_d = 0.1L, 0.3L$, and $0.5L$ are considered for the delamination. Table 3 shows that the fundamental frequency of the non-actuated microbeam ($V_s = 0$) decreases when the delamination occurs near the center of the microbeam. The fundamental frequency behavior versus different applied DC voltage is illustrated in Fig. 10 which shows the pull-in voltage decreases when the lengthwise delamination comes near to the center of the microbeam. Also, both of these observations show that the vibration response

Table 3. The fundamental frequency of the delaminated microbeam with various horizontal location ($h_2 = 0.5h$ and $L_d = 0.1L$) at rest ($V_s = 0$).

Lengthwise location, X_d	$0.5L$	$0.3L$	$0.1L$
Fundamental frequency [KHz]	95.980	95.980	100.593

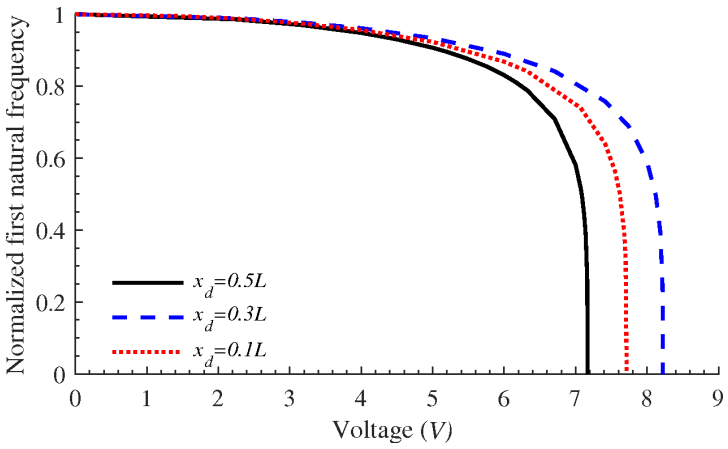

Fig. 10. The effect of delamination lengthwise location on the fundamental frequency of the microbeam ($h_2 = 0.5h$ and $L_d = 0.1L$).

related to different lengthwise location is not regular such as static response shown in last section.

Finally, the classical theory limitation to be responsible for the fundamental frequency behavior of four different microbeams with the various thicknesses and the constant $b/h = 22.5$ and $L/h = 200$ are studied. The fundamental frequency of the non-actuated microbeam ($V_s = 0$) is shown in Table 4. It is observed that the difference between the two models is significant for the thin microbeam ($h < 10l$). Figure 11 shows the prediction of the fundamental frequency variation versus different applied voltage of the two models. The results show that the classical theory does not exactly predict the behavior of the thin microbeam with the ratio of the thickness to the length scale parameter below 10. In this condition, the exact pull-in voltage is just obtained using non-classical theory. Also, it is observed that the classical theory is approximately responsible for the behavior of the microbeam with the h/l ratio lower than 10 and near to 6 (Fig. 11c) just below the pull-in instability operation. But only the non-classical theory should be used to study for the very thin microbeam with $h < 10l$ in all applied voltage.

Table 4. The fundamental frequency prediction of the delaminated microbeam by using two models ($L_d = 0.1L$, $h_2 = 0.5h$, $x_d = 0.5L$, $b = 22.5h$, and $L = 200h$) at rest ($V_s = 0$).

Microbeam thickness, h	$2l$	$4l$	$6l$	$10l$	$20l$
Classical fundamental frequency [KHz]	550.134	275.067	183.378	110.027	55.013
Non-Classical fundamental frequency [KHz]	876.896	328.234	200.632	113.985	55.523

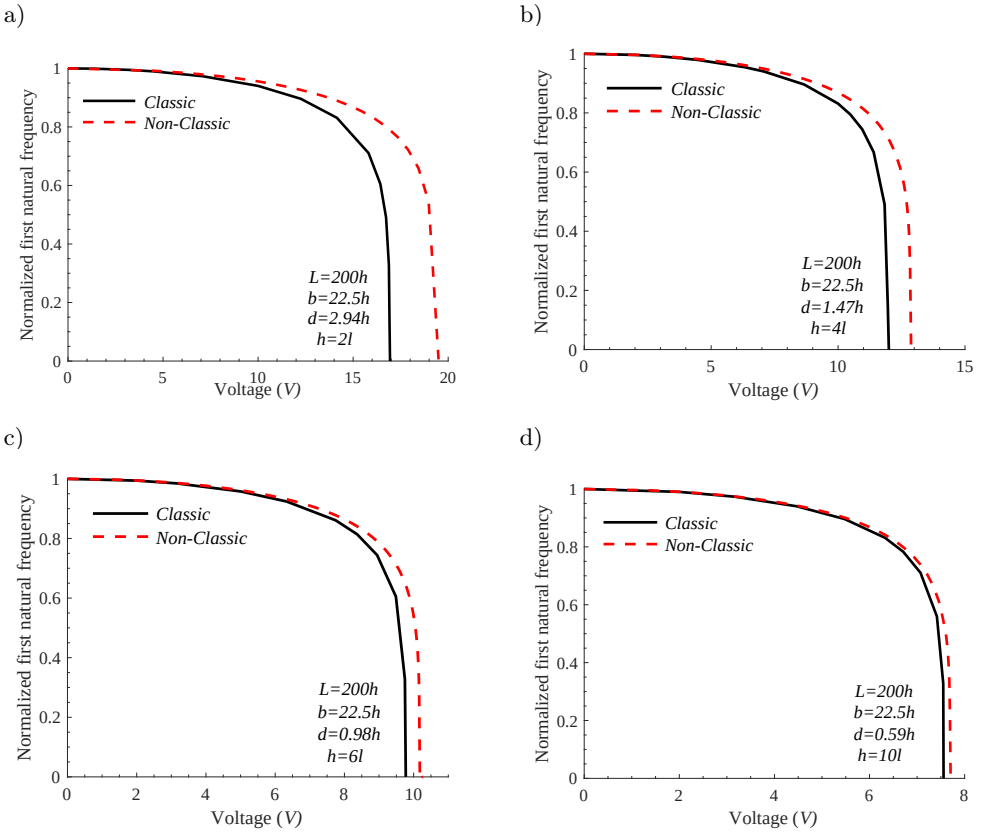

FIG. 11. The normalized fundamental frequency of the delaminated microbeam ($x_d = 0.5L$, $h_2 = 0.5h$, and $L_d = 0.1L$) based on the classical and the non-classical theory with various thickness; a) $h = 2l$, b) $h = 4l$, c) $h = 6l$ and d) $h = 10l$.

7. Conclusion

In this paper, the delamination effect on the static response, free and forced vibrational characteristics of a microbeam was studied. The delaminated microbeam was divided into four intact sub-beams. The non-classical Euler–Bernoulli model along with the constrained mode model was considered to obtain the mathematical formulations of the delaminated microbeam. The well-known Galerkin's method was used to convert the partial differential equations of motion into the ordinary differential equations. The results for the intact microbeam was validated against the result reported from the available literature and 3D electromechanical simulation result and then the excellent agreements were observed. Numerical results were obtained to investigate the influence of the different parameters of the delamination on the microbeam's response. It was shown that remarkable variation occurred in the natural frequency and static response

of the delaminated microbeam which is very important for nondestructive detection of the delamination in microbeam. Also, the difference between two classical and non-classical models of the Euler–Bernoulli beam was investigated using the study on the delaminated beam with a different geometry. The results show that only the non-classical theory should be used to study for the very thin microbeam with thickness lower than $10l$ in all applied voltage.

Acknowledgements

The authors acknowledge the funding support of the Babol Noshirvani University of Technology through the grant program No. BNUT/370557/98.

References

1. R. Kumar, R. Kumar, *Effects of phase lags on thermoelastic damping in micro-beam resonators*, International Journal of Structural Stability and Dynamics, 2019.
2. S. Molaei, B.A. Ganji, *Design and simulation of a novel RF MEMS shunt capacitive switch with low actuation voltage and high isolation*, Microsystem Technologies, **23**, 6, 1907–1912, 2017.
3. A. Razeghi, B.A. Ganji, *A novel design of RF MEMS dual band phase shifter,* Microsystem Technologies, **20**, 3, 445–450, 2014.
4. E.M. Abdel-Rahman, M.I. Younis, A.H. Nayfeh, *Characterization of the mechanical behavior of an electrically actuated microbeam*, Journal of Micromechanics and Microengineering, **12**, 6, 759, 2002.
5. M.I. Younis, E.M. Abdel-Rahman, A. Nayfeh, *A reduced-order model for electrically actuated microbeam-based MEMS*, Journal of Microelectromechanical systems, **12**, 5, 672–680, 2003.
6. M. Naoui, H. Samaali, F. Najar, *Modeling and design of very low-voltage mems microswitch using dynamic pull-in*, 2015 IEEE 12th International Multi-Conference on Systems, Signals & Devices (SSD15), pp. 1–3, 2015.
7. S. Chaterjee, G. Pohit, *A large deflection model for the pull-in analysis of electrostatically actuated microcantilever beams*, Journal of Sound and Vibration, **322**, 4-5, 969–986, 2009.
8. M. Moghimi Zand, M. Ahmadian, *Dynamic pull-in instability of electrostatically actuated beams incorporating Casimir and van der Waals forces*, Proceedings of the Institution of Mechanical Engineers, Part C: Journal of Mechanical Engineering Science, **224**, 9, 2037–2047, 2010.
9. M. Mojahedi, M.M. Zand, M. Ahmadian, *Static pull-in analysis of electrostatically actuated microbeams using homotopy perturbation method*, Applied Mathematical Modelling, **34**, 4, 1032–1041, 2010.
10. B. Wang, J. Zhao, S. Zhou, *Micro scale Timoshenko beam model based on strain gradient elasticity theory*, European Journal of Mechanics-A/Solids, **29**, 4, 591–599, 2010.

11. B. WANG, S. ZHOU, J. ZHAO, X. CHEN, *Size-dependent pull-in instability of electrostatically actuated microbeam-based MEMS*, Journal of Micromechanics and microengineering, **21**, 2, 027001, 2011.

12. K. WANG, B. WANG, *Influence of surface energy on the non-linear pull-in instability of nano-switches*, International Journal of Non-Linear Mechanics, **59,** 69–75, 2014.

13. K. WANG, T. KITAMURA, B. WANG, *Nonlinear pull-in instability and free vibration of micro/nanoscale plates with surface energy–a modified couple stress theory model*, International Journal of Mechanical Sciences, **99**, 288–296, 2015.

14. K. WANG, B. WANG, *A general model for nano-cantilever switches with consideration of surface effects and nonlinear curvature*, Physica E: Low-dimensional Systems and Nanostructures, **66**, 197–208, 2015.

15. E.M. MIANDOAB, A. YOUSEFI-KOMA, H.N. PISHKENARI, *Poly silicon nanobeam model based on strain gradient theory*, Mechanics Research Communications, **62**, 83–88, 2014.

16. E.M. MIANDOAB, H.N. PISHKENARI, A. YOUSEFI-KOMA, H. HOORZAD, *Polysilicon nano-beam model based on modified couple stress and Eringen's nonlocal elasticity theories*, Physica E: Low-dimensional Systems and Nanostructures, **63**, 223–228, 2014.

17. M.H. JALALI, O. ZARGAR, M. BAGHANI, *Size-dependent vibration analysis of FG microbeams in thermal environment based on modified couple stress theory*, Iranian Journal of Science and Technology, Transactions of Mechanical Engineering, **43**, 761–771, 2019.

18. S. BHATTACHARYA, D. DAS, *Free vibration analysis of bidirectional-functionally graded and double-tapered rotating micro-beam in thermal environment using modified couple stress theory*, Composite Structures, **215**, 471–492, 2019.

19. M.A. ATTIA, R.A. SHANAB, S.A. MOHAMED, N.A. MOHAMED, *Surface energy effects on the nonlinear free vibration of functionally graded Timoshenko nanobeams based on modified couple stress theory*, International Journal of Structural Stability and Dynamics, **19**, 11, 1950127, 2019.

20. Ç. MOLLAMAHMUTOĞLU, A. MERCAN, *A novel functional and mixed finite element analysis of functionally graded micro-beams based on modified couple stress theory*, Composite Structures, **223**, 110950, 2019.

21. R.A. SHANAB, S.A. MOHAMED, N.A. MOHAMED, M.A. ATTIA, *Comprehensive investigation of vibration of sigmoid and power law FG nanobeams based on surface elasticity and modified couple stress theories*, Acta Mechanica, **34**, 1, 2020.

22. J. WANG, Y. LIU, J. GIBBY, *Vibrations of split beams*, Journal of Sound and Vibration, **84**, 4, 491–502, 1982.

23. P.M. MUJUMDAR, S. SURYANARAYAN, *Flexural vibrations of beams with delaminations*, Journal of Sound and Vibration, **125**, 3, 441–461, 1988.

24. M.-H. SHEN, J. GRADY, *Free vibrations of delaminated beams*, AIAA Journal, **30**, 5, 1361–1370, 1992.

25. C.N. DELLA, D. SHU, P. MSRAO, *Vibrations of beams with two overlapping delaminations*, Composite Structures, **66**, 1, 101–108, 2004.

26. E. MANOACH, J. WARMINSKI, A. MITURA, S. SAMBORSKI, *Dynamics of a composite Timoshenko beam with delamination*, Mechanics Research Communications, **46**, 47–53, 2012.

27. M.H. Kargarnovin, M.T. Ahmadian, R.A. Jafari-Talookolaeia, *Forced vibration of delaminated Timoshenko beams subjected to a moving load*, Science and Engineering of Composit Materials, **19**, 2, 145–157, 2012.

28. R.-A. Jafari-Talookolaei, M.H. Kargarnovin, M.T. Ahmadian, *On the dynamic response of a delaminated composite beam under the motion of an oscillating mass*, Journal of Composite Materials, **46**, 22, 2863–2877, 2012.

29. M. Kargarnovin, R. Jafari-Talookolaei, M. Ahmadian, *Vibration analysis of delaminated Timoshenko beams under the motion of a constant amplitude point force traveling with uniform velocity*, International Journal of Mechanical Sciences, **70**, 39–49, 2013.

30. R.-A. Jafari-Talookolaei, N. Ebrahimzade, S. Rashidi-Juybari, K. Teimoori, *Bending and vibration analysis of delaminated Bernoulli–Euler micro-beams using the modified couple stress theory*, Scientia Iranica, **25**, 2, 675–688, 2018.

31. S. Park, X. Gao, *Bernoulli–Euler beam model based on a modified couple stress theory*, Journal of Micromechanics and Microengineering, **16,** 11, 2355, 2006.

32. M. Joglekar, D. Pawaskar, *Closed-form empirical relations to predict the static pull-in parameters of electrostatically actuated microcantilevers having linear width variation*, Microsystem Technologies, **17**, 1, 35–45, 2011.

33. A. Bhushan, M. Inamdar, D. Pawaskar, *Simultaneous planar free and forced vibrations analysis of an electrostatically actuated beam oscillator*, International Journal of Mechanical Sciences, **82**, 90–99, 2014.

34. B. Choi, E. Lovell, *Improved analysis of microbeams under mechanical and electrostatic loads*, Journal of Micromechanics and Microengineering, **7**, 1, 24, 1997.

35. S.B. Sedaghat, B.A. Ganji, *A novel MEMS capacitive microphone using spring-type diaphragm*, Microsystem Technologies, **25**, 1, 217–224, 2019.

36. B.G. Kiral, *Free vibration analysis of delaminated composite beams*, Science and Engineering of Composite Materials, **16**, 3, 209–224, 2009.

37. R.-A. Jafari-Talookolaei, M. Abedi, *Analytical solution for the free vibration analysis of delaminated Timoshenko beams*, The Scientific World Journal, **2014**, 280256, 2014.

Received November 13, 2019; revised version April 5, 2020.
Published online April 30, 2020.